ELSEVIER

Journal of Chromatography A, 744 (1996) 45–54

JOURNAL OF CHROMATOGRAPHY A

Preparative capillary electrophoresis with wide-bore capillaries

Hongfeng Yin*, Catherine Keely-Templin, Douglass McManigill

Hewlett-Packard Laboratories, 3500 Deer Creek Road, Bldg. 26U, Palo Alto, CA 94304, USA

Abstract

Sample load is in proportion to the square of capillary inner diameter in capillary electrophoresis (CE). With wide-bore capillaries, single run fraction collection of CE often gives enough material for further identification techniques, such as matrix-assisted laser desorption ionization time-of-flight (MALDI-TOF) MS and peptide sequencing. Limitations of using wide bore capillaries for CE and solutions to them are discussed in this investigation. An existing CE instrument has been modified in order to use wide-bore capillaries. Tryptic digest peptides have been identified with off-line wide bore CE–MALDI-TOF-MS techniques.

Keywords: Preparative electrophoresis; Capillary columns; Peptides

1. Introduction

Fifteen years after its first introduction, capillary electrophoresis (CE) has found wide acceptance in the analytical sciences, with application in diverse fields, including pharmaceutical analysis and bioscience research. Frequently CE has been called upon to provide semi-preparative quantities for further analysis, such as for microsequencing or mass spectrometry analysis. Bundled capillaries, multiple injections combined with fraction collection, and larger capillaries have all been used with some success to provide nanomolar quantities of analytes, but these approaches have for the most part resulted in reduced performance of the CE system. Clearly the need exists for capillary separation methods to more closely match the input loading requirements of the analytical techniques with which they are mated.

While it is possible to inject greater volumes into standard 75 μm CE capillaries for increased sample loading, this can only be used to a very limited degree. The increased injection plug variance due to this increased injection volume will soon become the dominating plate height contributor. Separation efficiency will suffer since the limiting efficiency of capillary systems is determined by the ratio of the injected volume to the analytical volume of the system. Fig. 1A and B illustrates this problem; in a 75 μm I.D. capillary a 46 nl injection volume (10 mm injection plug length) will effectively destroy the separation. However, this same volume injected into a larger diameter capillary will have a less detrimental effect, as the ratio of injection volume to analytical volume may remain the same or possibly even decrease. Increasing the inside diameter (I.D.) of the capillary allows the injected volume to increase as the square of the diameter, with no increase in injection plug length. For example, an increase in capillary diameter, from 75 to 180 μm, would increase the injected volume by a factor of six with no change in injection plug length and therefore with no change in separation efficiency (Fig. 1A and C). Injection volumes of up to 138 nl (5.4 mm plug length) have been tested, with only minimal degradation of separation efficiency (Fig. 1D).

Many experimental studies have indicated rapid

*Corresponding author.

0021-9673/96/$15.00
PII S0021-9673(96)00424-4

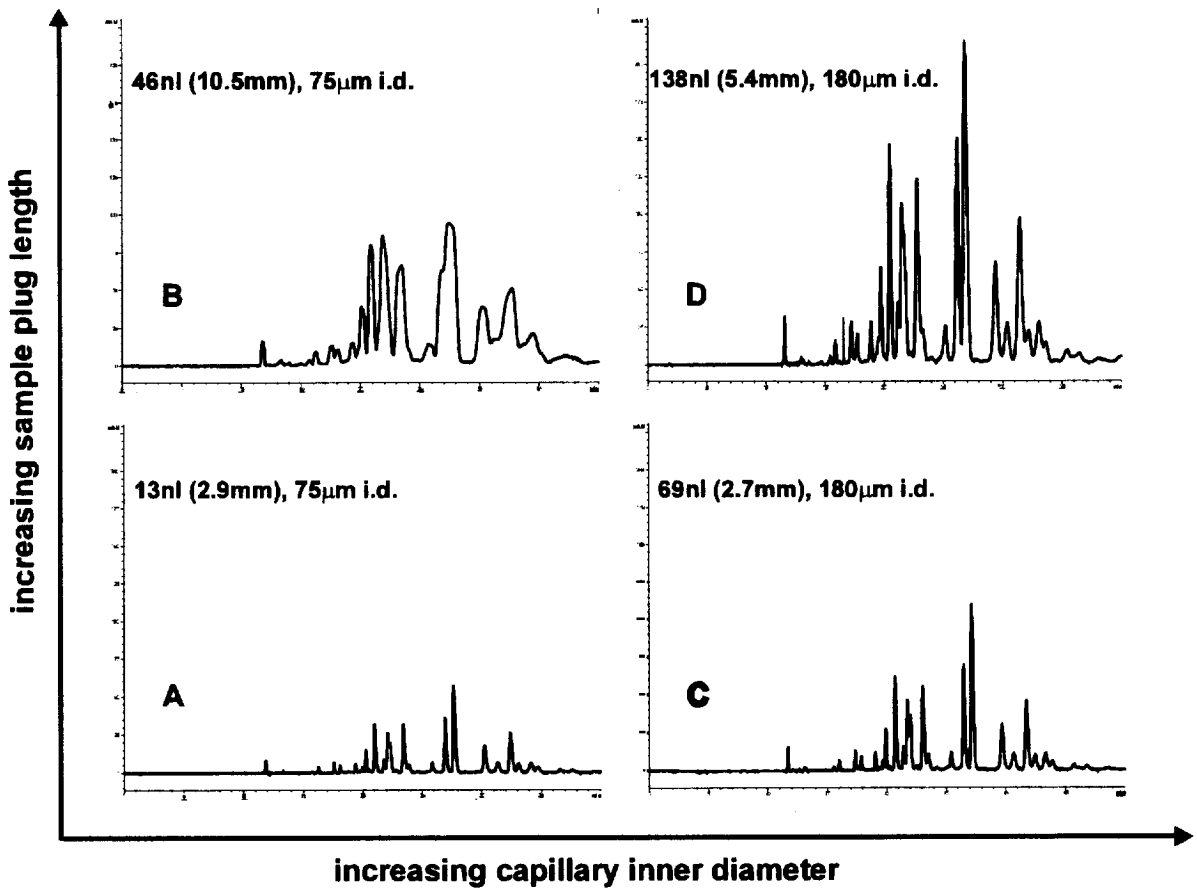

Fig. 1. CE separation of rhGH tryptic digest as a function of increasing sample plug length (Volume) and capillary I.D.

decreases in separation efficiency when either of these two approaches are attempted. Additionally, theoretical studies suggest several mechanisms by which band broadening may quickly increase in large bore capillaries:

- Siphoning between electrode reservoirs.
- Temperature effects due to Joule heat, including both radial temperature profile and average buffer temperature.
- pH changes within the buffer reservoirs due to the increased electrical current.

This investigation has attempted to consider these mechanisms individually in wide-bore capillaries, and to develop practical solutions which could result in successful separations on such capillaries. Results demonstrate (Fig. 2) that, with appropriate attention to these factors, acceptable system performance is quite feasible, and that the increased loadability of wide-bore capillaries permits much more practical injection volumes when fraction collection is required.

2. Experimental

2.1. Apparatus

All CE separations and fraction collections were performed on HP1600A HP^{3D}CE system from

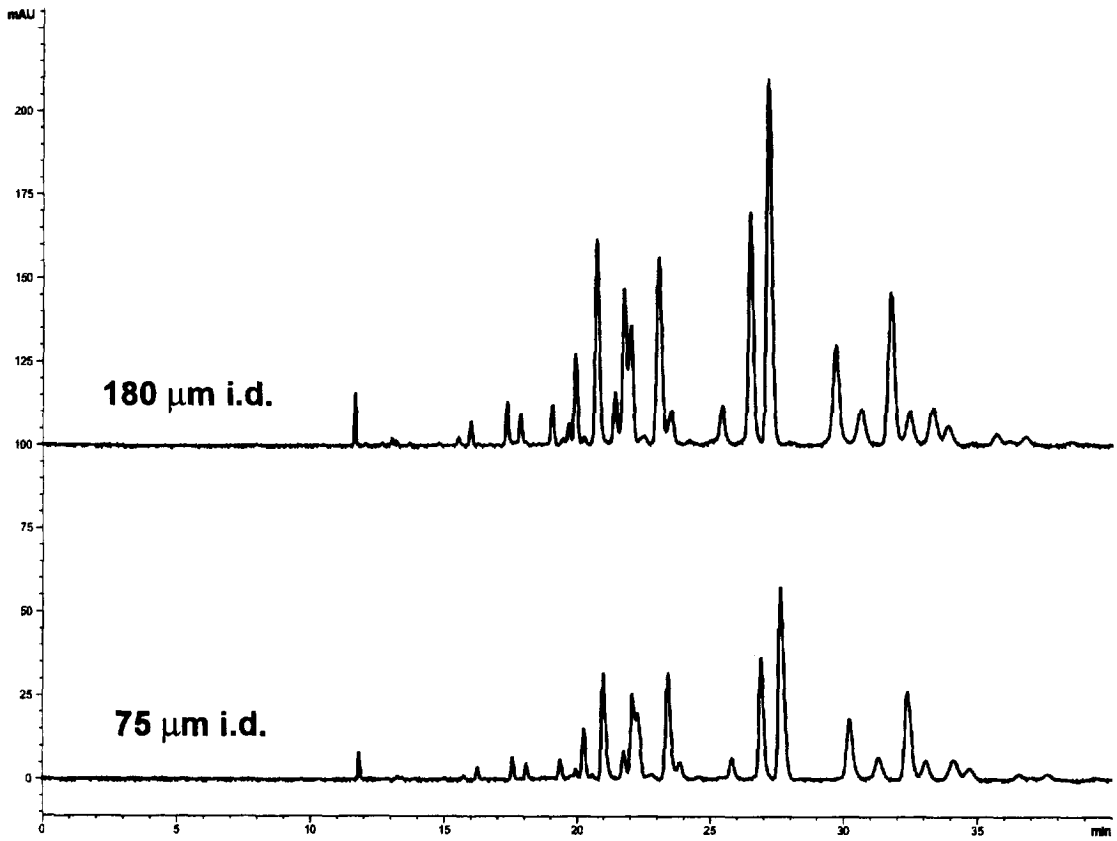

Fig. 2. CE separation of rhGH tryptic digest with 75 μm and 180 μm I.D. capillaries, showing that column performance remains high with increasing diameter and sample load.

Hewlett-Packard (Waldbronn, Germany). Hydrodynamic sample injection was accomplished by applying pressure at the injection end of the capillary. The CE system integrates injection pressure over injection time, so that sample plug length can be precisely controlled. Buffer reservoirs were filled with buffer by its automatic buffer replenishment system. CE separations were performed in constant current mode at 300 μA for 180 μm I.D. capillaries and 52 μA for 75 μm I.D. capillaries. Forced air cooling was used to control capillary temperature. UV absorbance was detected with the system's diode array detector. Signals at 200 nm were displayed in this paper.

HP 2030A MALDI-TOF-MS (Hewlett-Packard, Palo Alto, CA, USA) was used to analyze the collected CE fractions, with HP 2039A (2,5-dihydoxybenzoic acid) as matrix.

2.2. Reagents

100 m*M* CE buffer was prepared with monobasic potassium phosphate (J.T. Baker, Philipsburg, NJ, USA). The pH was then adjusted to 2.0 with phosphoric acid (Sigma, St. Louis, MO, USA). Tryptic digests of rhGH (recombinant human growth hormone) and rtPA (recombinant tissue plasminogen activator) were provided by Genentech (South San Francisco, CA, USA).

Restrictors at the ends of 180 μm I.D. fused-silica capillaries (PolyMicro Technology, Phoenix, AZ, USA) were formed by heating the capillary ends. A

electric discharge device (Orionics, Bozeman, MT, USA) was used to generate an electrical arc discharge around the capillary ends, so that they were heated to near melting temperature, thus closing the ends.

3. Results and discussion

3.1. Siphoning in wide-bore capillaries

When using wide-bore capillaries, flow through the capillary due to siphoning can be significant in that it can cause large changes in velocity and can increase band broadening, since it is pressure-driven flow. This effect was examined theoretically and experimentally, and it was found that by modifying the capillary with flow restrictors, siphoning effects were greatly reduced.

3.1.1. Theory

The change in velocity will vary linearly with the pressure head, and with the square of the diameter in a normal capillary [1–3] (Eq. 1). The plate height function is more complicated, but in wider-bore capillaries, plate height will increase linearly with pressure, and with the fourth power of the diameter (Eq. 2). Thus it is expected that siphoning can severely impact the separation efficiency in wide-bore capillaries.

$$\Delta v(r, p) = \frac{p r_i^2}{8\eta L}(1 - 2r^2) \tag{1}$$

$$H = \frac{2}{\hat{u}} K_d \tag{2}$$

$$K_d = D - \frac{2r_i^2}{D} \times \int_0^1 \left\{ \int_0^r \frac{1}{r'} \left[\int_0^{r'} \Delta v(r'') r'' \mathrm{d}r'' \right] \mathrm{d}r' \right\} \Delta v(r) r \mathrm{d}r$$

Fig. 5 gives the theoretical plate height as a function of velocity for a 50 cm straight 180 μm I.D. capillary, assuming that only diffusion and the pressure flow profile contribute to plate height. The three curves represent different amounts of siphoning via pressure heads (inlet above outlet): 0 mm, 2 mm (0.2 mbar), and 4 mm (0.4 mbar). As expected, even a small pressure head causes enough siphoning to greatly increase the plate height in this column. By comparison, the pressure head would have to be 30 mm (3 mbar) in a 75 μm I.D. capillary to generate the plate heights given in the 0.2 mbar curve.

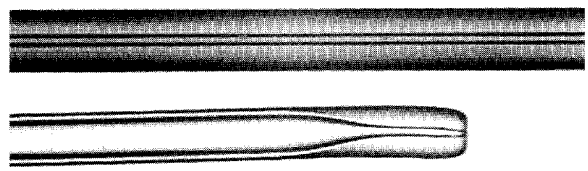

Fig. 3. 50 μm I.D. straight capillary and 180 μm I.D. capillary with 50 μm I.D., 0.5 mm long restrictor formed at the end.

To reduce siphoning, the ends of the wide-bore capillaries were fire polished to form a short restriction 0.5 mm long and with an I.D. of 50 μm (Fig. 3). This worked well to reduce the effects of siphoning to an acceptable amount, comparable to a 135 μm I.D. capillary. The buffer replenishment feature of the HP^{3D}CE apparatus permits buffer leveling of the electrode reservoirs, which together with the modified capillaries resulted in improved reproducibility of the migration time and peak area, as well as enabling better control of pressure injections and fraction collection.

Fig. 4 shows demonstration separation in a 180 μm restricted capillary with imposed pressure head of 0 mm, 2 mm and 4 mm. The velocity and plate heights calculated from the indicated peaks are plotted in Fig. 5, where it can be seen that they are indeed much lower than the theoretical curves for the non-restricted capillary. In fact, this experiment could not be run on a straight bore capillary due to

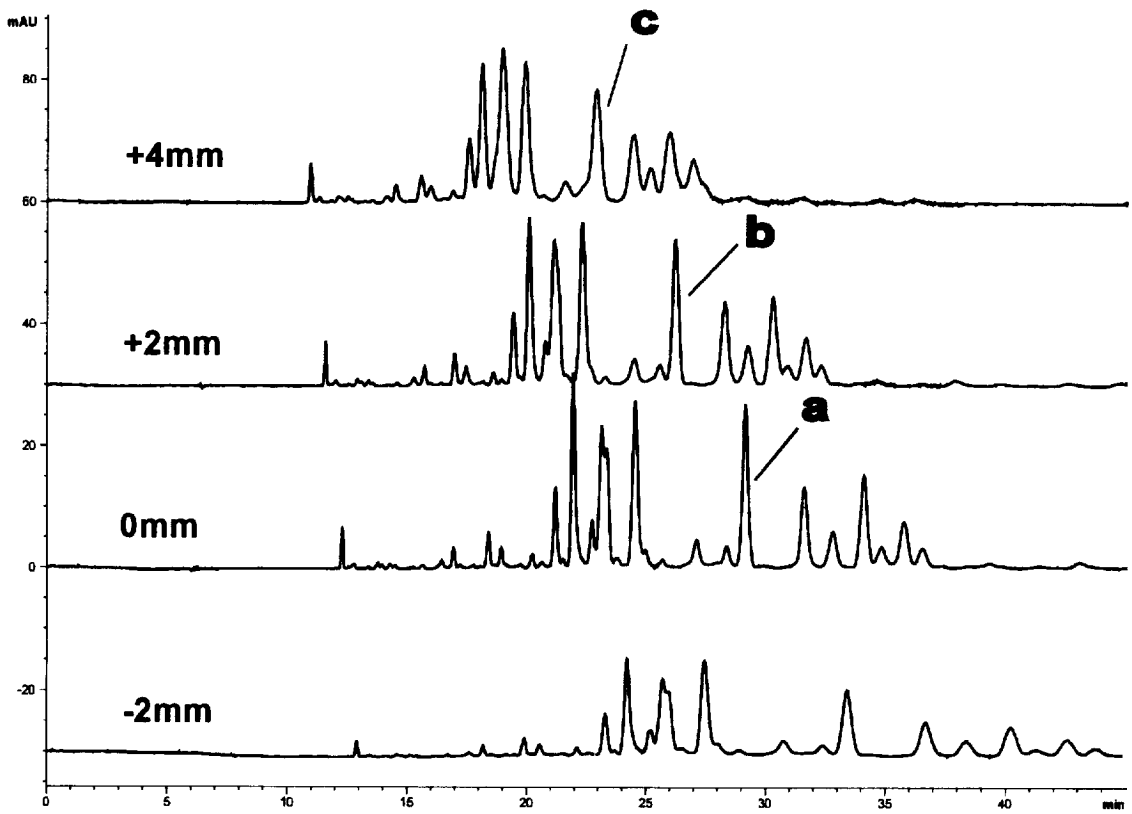

Fig. 4. Separation of rhGH tryptic digest with restricted 180 μm capillary at different pressure heads, showing effect of pressure flow on separation.

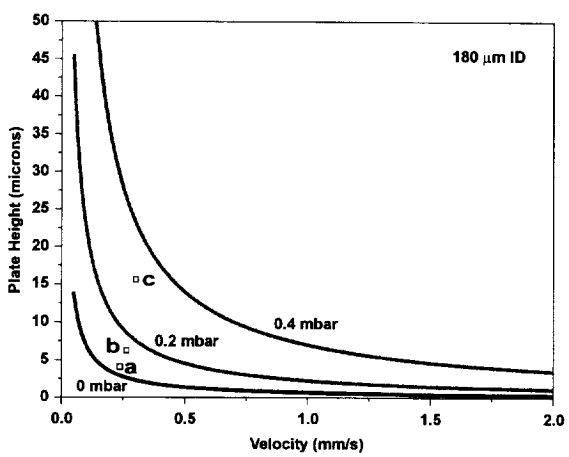

Fig. 5. Plate height as a function of velocity with differing amounts of siphoning pressure. Theoretical curves for 180 μm I.D. straight capillary and data points (□) are for a restricted 180 μm I.D. capillary.

siphoning effects at the injection, and huge changes in migration time.

3.2. Temperature effects

For a given applied CE voltage, the electrical current through the capillary increases with the square of the diameter, thus average length wide-bore capillaries in CE require a larger electrical current, which leads to large power dissipation in the capillary. This power is dissipated as Joule heating, and leads to a radial temperature gradient and an increased average temperature. This has been thought to cause significant band broadening, but here we examine the theory and run experiments to show that for peptide sized molecules the actual increase in plate height is negligible.

3.2.1. Radial temperature profile

The radial temperature gradient is a function of the power dissipated, capillary dimensions, thermal characteristics of the buffer and capillary, and the external temperature, and can be calculated [4] (Eq. 3). Fig. 6 shows the thermal profiles for 180 μm and 75 μm I.D. capillaries with the external temperature assumed to be 45°C. While the 180 μm gradient is much larger than that of the 75 μm, there is still only 1.2°C difference between the outside wall and the center.

$$T(r) = \frac{J_0(\beta r)}{J_0(\beta r_i)} \left[T_0 + \frac{1}{\mu} + \frac{w_t}{2\pi k_2} \ln\left(\frac{r_o}{r_i}\right) \right] - \frac{1}{\mu} \quad (3)$$

with

$$w_t = \left[\frac{2\pi\mu w_o r_i k_2 J_1(\beta r_i)}{\beta k_2 J_0(\beta r_i) - \mu w_0 r_i \ln\left(\frac{r_o}{r_i}\right) J_1(\beta r_i)} \right] \times \left(T_0 + \frac{1}{\mu}\right)$$

$$\beta = \sqrt{\frac{\mu w_0}{k_1}}$$

$$\mu = -\alpha$$

The resultant plate height can be calculated by assuming the temperature profile causes a viscosity profile which in turn causes a parabolic velocity profile (Eq. 2 and Eq. 4).

$$\Delta v(r, \Delta T) = \frac{\mu \Delta T \hat{u}}{2}(1 - 2r^2) \quad (4)$$

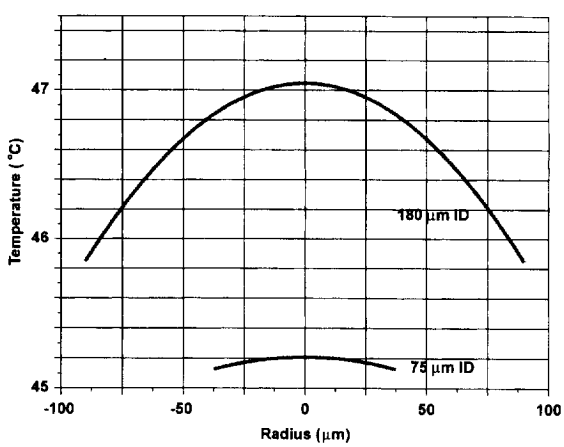

Fig. 6. Theoretical temperature profile inside capillary, as a function of capillary inside radius.

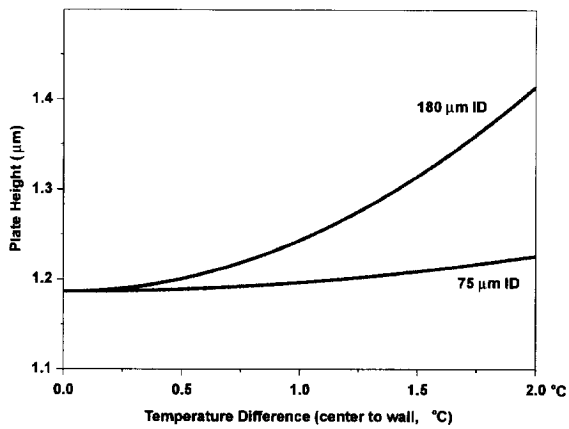

Fig. 7. Theoretical plate height due to radial temperature profile, see text.

Fig. 7 shows plate height as a function of the difference in temperature between the wall and the center, assuming the velocity changes 2% per°C and assuming a diffusion coefficient representative of peptides. As can be seen, while the contribution is much greater for a 180 μm capillary than for a 75 μm one, it is still less than 0.1 μm for the predicted temperature difference of 1.2°C. This contribution will be negligible, especially when the contribution to plate height due to the finite injection volume is taken into account.

In a system which has siphoning in addition to a temperature profile, the increase in plate height will be greater than the sum of the two plate height effects because the profiles will interact with each other. This will not be explored here since we have reduced the siphoning, but it should be kept in mind.

3.2.2. Average buffer temperature

Three watts, dissipated in a 375 μm O.D.×180 μm I.D. capillary will raise the average temperature inside the capillary by about 20°C over the control temperature when forced air cooling is

used. Furthermore, mounting and sealing points inaccessible to cooling may form hot spots where the buffer may boil. Fixture designs that allow proper cooling can minimize hot spots, but we will now examine how the average temperature effects the CE separation.

Fig. 8 shows separations run in a restricted 180 μm I.D. capillary with the control temperature held at 25°C and also in a 75 μm I.D. capillary with control temperatures of 25°C, 35°C and 45°C. Comparison of the velocities and efficiencies indicates that the inside of the 180 μm, 25°C capillary is approximately the same temperature as the 75 μm, 45°C capillary.

Note that there is no significant difference in band broadening between the four runs, indicating that the average temperature increase is not a problem for this separation. This figure also supports the theoretical prediction that the temperature gradient effect on plate height is negligible.

3.3. Buffer depletion due to coulombic titration

Because up to 300 μA current is routinely applied for wide-bore capillary electrophoresis, buffer depletion due to coulombic titration occurs much faster than in standard capillaries. For example, Table 1 shows the pH change of 100 m*M* pH 2.5 phosphate buffer during electrophoresis for given volumes of buffer when 300 μA current is applied. To reduce buffer depletion, 4–5 ml triple vials were constructed (Fig. 9). Using these vials, a two hour run at 300 μA resulted in a buffer pH change of less than 0.1 pH units.

Tryptic digest of rtPA was separated with a modified 180 μm I.D. capillary (Fig. 10). The

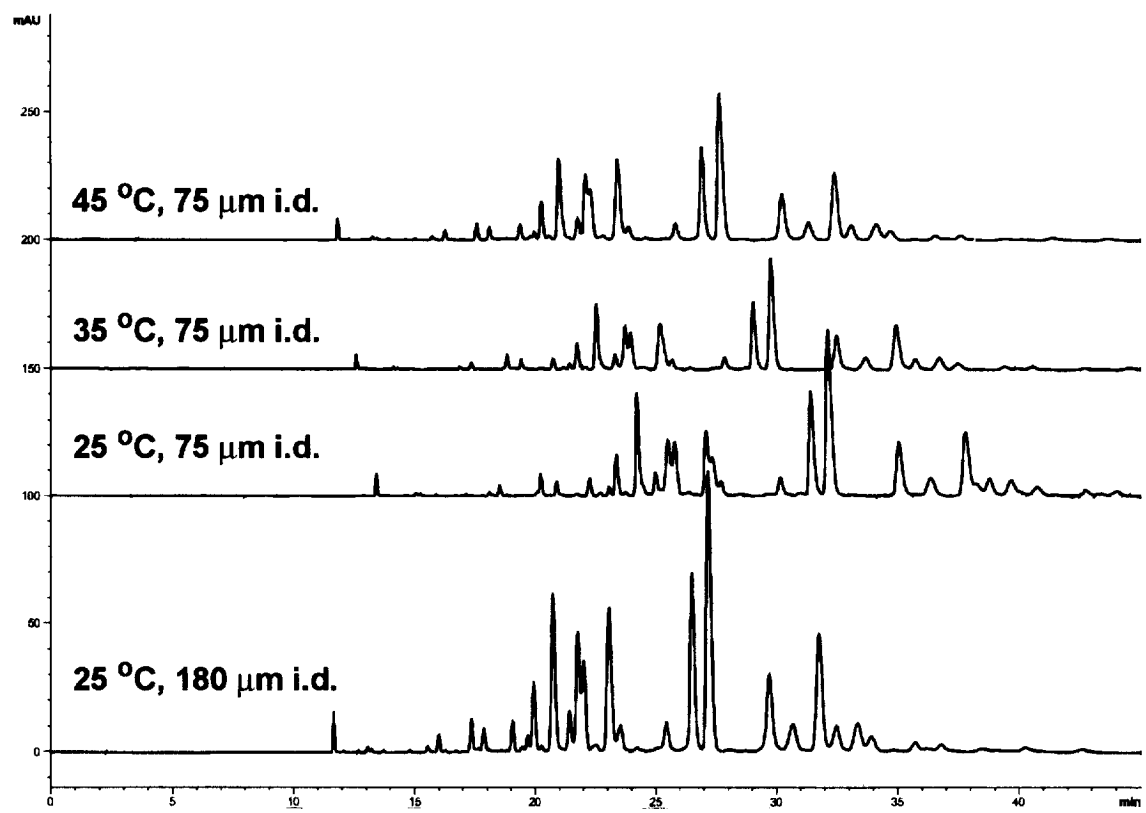

Fig. 8. Separation of rhGH tryptic digest with 180 μm I.D. capillary at 25°C and with 75 μm I.D. capillary at 25, 35 and 45°C, showing effect of average temperature on separation speed.

Table 1
Changes of pH due to buffer electrode processes, as a function of the volume of 100 m*M* buffer and the time in which a 300 μA current is applied

Volume (ml)	30.0 min	60.0 min	90.0 min	120.0 min
0.5	0.198	0.420	0.709	1.268
1.0	0.098	0.198	0.304	0.420
2.0	0.049	0.098	0.148	0.198
4.0	0.024	0.049	0.073	0.098

fraction marked with a box was collected from the capillary using 25 mbar pressure for 12 s. MALDI-TOF-MS analysis identified this fraction as a glycopeptide fragment (T45) of the rtPA digest (Fig. 11). The large sample volume injections allow complex samples to be analyzed with adequate material in the individual peaks to permit subsequent analysis, without sacrificing resolution.

4. Conclusions

This investigation has focused on the role of capillary diameter in CE separations, and whether practical solutions to attendant problems can be implemented. Experimental data has been generated, supported by theory, which demonstrate that

- The effects of siphoning can be severe, but with appropriate instrument and column design can be controlled.
- Radial temperature profile has less of an effect than expected, if all contributions to plate height are considered.
- Average temperature increases due to the increased joule heating are less important than proper thermal design of the total column.

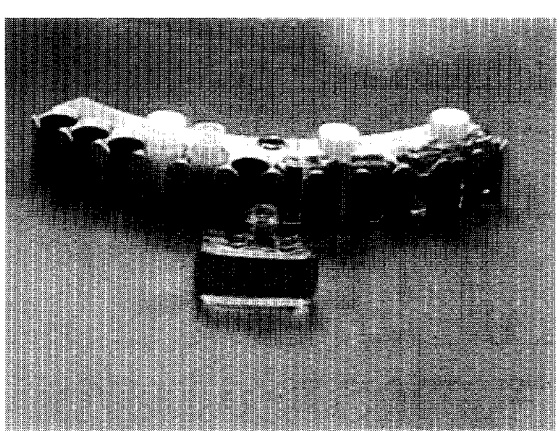

Fig. 9. Modification to the HP^{3D}CE sample tray and triple-vials.

The increased loadability of CE columns may in the future permit a more complimentary match between HPCE and emerging micro LC systems, interfacing techniques for hyphenated instruments, and semi-preparative sample production. This in turn may allow the possibility of a unified apparatus for micro separations work of high sensitivity and separation efficiency.

5. Nomenclature

D	Diffusion coefficient
H	Plate height
J_0, J_1	Bessel function of first kind, order 0 and 1
K_d	Total dispersion
k_1, k_2	Thermal conductivity of buffer and fused silica
L	Total length of capillary
p	Pressure
r	Normalized radius variable
r', r''	Integration variables representing r
r_i, r_o	Capillary radius, inside and outside
T_0	Temperature outside capillary
ΔT	Temperature difference, center to wall
$\hat{u}$	Average bulk velocity
Δv	Change in velocity function
w_0	Power dissipated
α	Temperature coefficient of resistivity
η	Viscosity of buffer
μ	$-\alpha$

Acknowledgments

rhGH and rtPA tryptic digest samples were kindly provided by Shiaw-Lin Wu and Yung-Fu Huang of Genentech Inc. MALDI-TOF-MS was done by John Chakel of HP Labs.

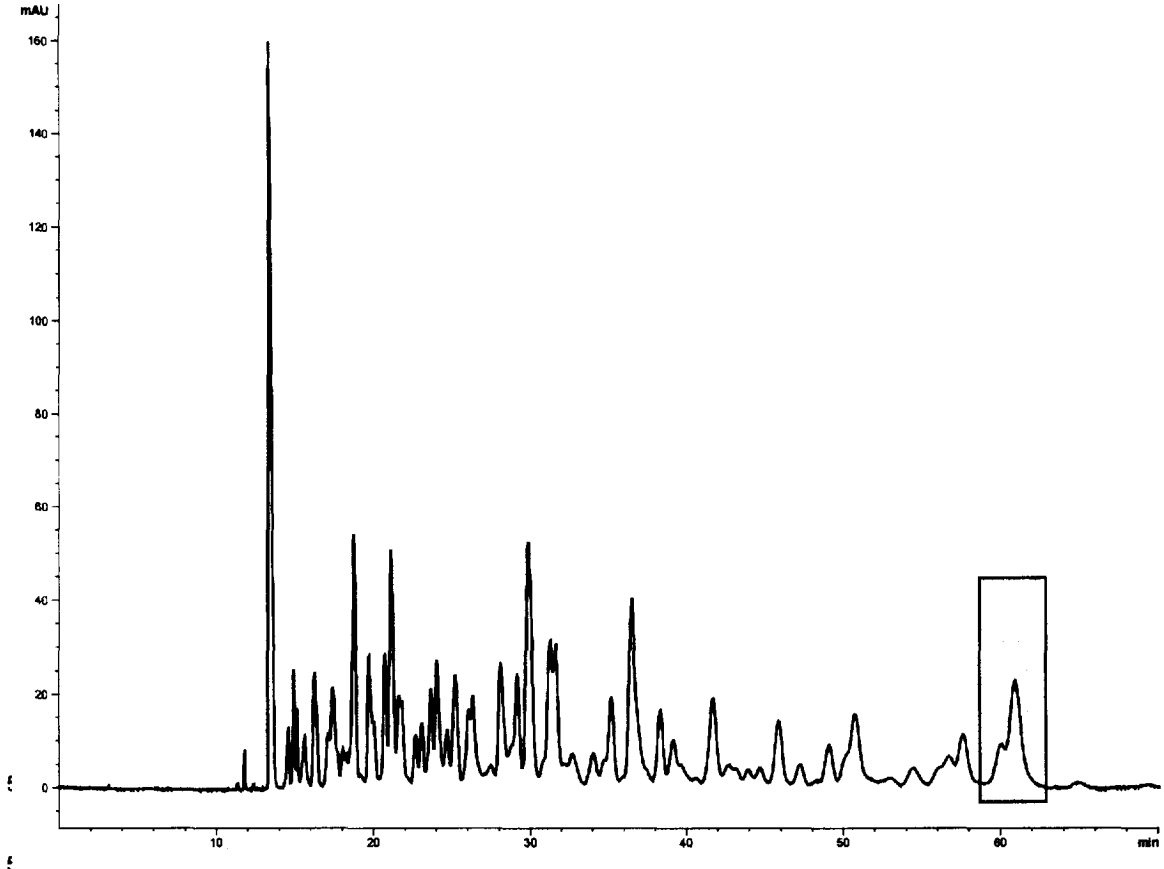

Fig. 10. CE separation of rtPA tryptic digest with fraction collection at boxed area.

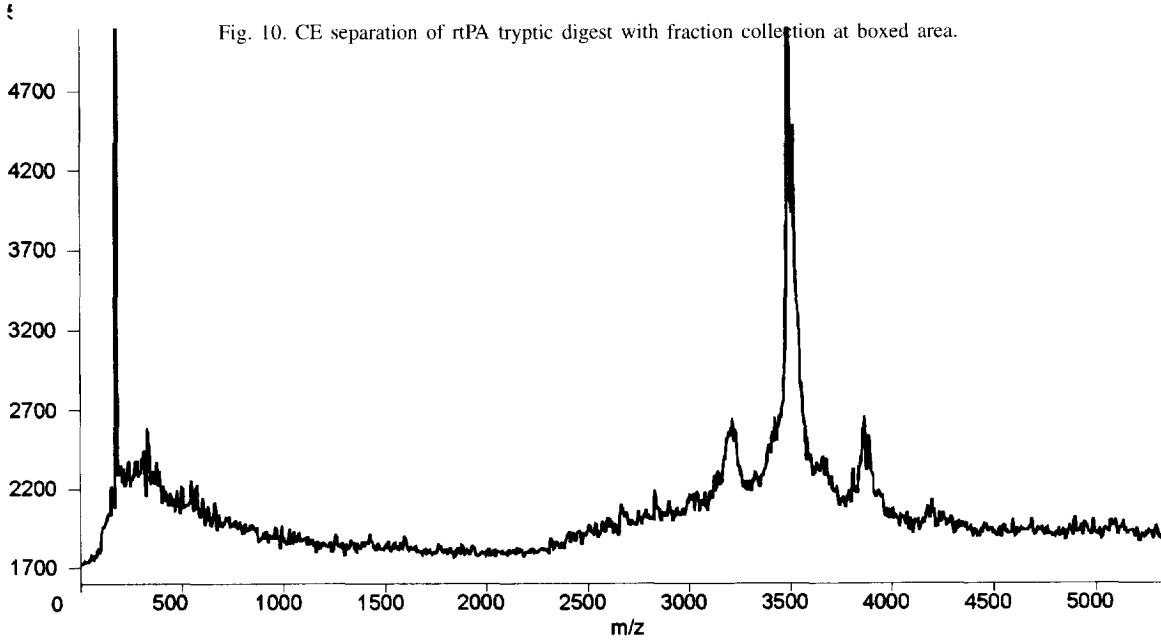

Fig. 11. MALDI-TOF mass spectrum of collected CE fraction.

References

[1] C.A. Keely, T.A. van de Goor and D. McManigill, Anal. Chem., 66 (1994) 4236–4242.
[2] R. Aris, Proc. R. Soc. London, A235 (1956) 66–77.
[3] R. Datta and V.R. Kotamarthi, AICHE J., 36 (1990) 916–926.
[4] J.F. Brown and J.O.N. Hinckley, J. Chromatogr., 109 (1975) 218–224.